Pergamon

Solar Energy, Vol. 54, No. 1, pp. 49–56, 1995

0038-092X/95 $9.50 + .00

0038-092X(94)00100-6

ADAPTIVE STRATEGIES USING STANDARD AND MIXED FINITE ELEMENTS FOR WIND FIELD ADJUSTMENT

G. WINTER, G. MONTERO, L. FERRAGUT,* and R. MONTENEGRO**
Centro de Investigación de Aplicaciones Numéricas en Ingeniería (CEANI), University of Las Palmas de Gran Canaria, Spain; *Department of Applied Mathematics and Informatic Methods, Polytechnic University of Madrid, Spain; **Department of Mathematics, University of Las Palmas de Gran Canaria, Spain

Abstract—In order to find a map of wind velocities, this study tries to obtain an incompressible wind field that adjusts to an experimental one: also verifying the corresponding boundary conditions of physical interest. This problem has been solved by several authors using finite differences or standard finite element techniques. In this paper, this problem is solved by two different adaptive finite element methods. The first makes use of standard finite element techniques, using linear interpolation of a potential function. In the second, a direct computation of the velocity field is undertaken by means of a mixed finite element method. Several error indicators are proposed for both formulations together with an adaptive strategy. We have applied both methods to several typical test problems, as well as to realistic data corresponding to the Island of Fuerteventura, with satisfactory results from a numerical point of view.

1. INTRODUCTION

In the past, the Methods of Finite Differences and Finite Elements have proved to be a useful tool for the computation of wind fields (see Adell *et al.*, 1987; Caneill *et al.*, 1984; Fraga *et al.*, 1985; Sherman, 1978). Nevertheless, to achieve a good accuracy the analysis requires a mesh, taking into account the field distribution and singularities due to boundary conditions and geometry.

In recent years there has been growing interest in assessing the reliability and quality of finite element solutions of problems arising in computational science and engineering. The use of *a posteriori* error estimates and error indicators has become an accepted tool for controlling such computational errors (see Babuska *et al.*, 1983).

A wind energy expert without a deep knowledge in numerical analysis can obtain reliable results using an adaptive finite element computer program as a "black box." Besides that, good error indicators allow one to adapt the mesh automatically, in order to obtain the solution of a given problem with optimal computational cost. Real time numerical simulation of wind fields is then possible.

The purpose of this paper is to describe the numerical simulation of wind fields by an adaptive finite element method. First, the problem using a classical mathematical model is solved in such a way that a Lagrange multiplier is calculated first and the velocity field is obtained by derivation. However, the computed field thus obtained is discontinuous through the faces of the finite elements (lines in 2D) and does not satisfy the incompressibility condition point-wise. Alternately, a direct computation of velocities is presented, using mixed finite elements. In this approach the numerical solution satisfies the incompressibility condition exactly.

For both models, standard and mixed finite elements, we propose several error indicators in order to automatically control the error of the numerical approximation. To improve the quality of numerical solutions we have adopted one of the most common techniques, that of h-refinement, which relies on subdivisions of a given type of finite element.

2. CLASSIC F.E.M. SOLUTION

2.1 *Mathematical model*

For a given bounded domain $\Omega \subset \mathbb{R}^d$ ($d = 2, 3$), with boundary $\Gamma = \Gamma_1 \cup \Gamma_2$, we look for a vectorial field $\mathbf{u}$ that adjusts, in a least square sense, to a wind field $\mathbf{u}_0$ obtained from the interpolation of experimental measurements and verifying the following equations:

$$\operatorname{div} \mathbf{u} = 0 \quad \text{in} \quad \Omega \tag{1}$$

$$\mathbf{u} \cdot \mathbf{n} = 0 \quad \text{on} \quad \Gamma_1 \tag{2}$$

where $\mathbf{n}$ is the vector, unitary and perpendicular to Γ_1, projecting from Γ.

The cost function will be,

$$J(\mathbf{u}) = \tfrac{1}{2} \int_\Omega (\mathbf{u} - \mathbf{u}_0)^t \mathbf{P} (\mathbf{u} - \mathbf{u}_0),$$

$\mathbf{P}$ being a diagonal matrix.

Then, the vectorial field $\mathbf{u}$ will be the solution of the problem: "Find $\mathbf{u} \in \mathbb{K}$ that verifies,

$$\left.\begin{aligned} J(\mathbf{u}) &= \min_{\mathbf{v} \in \mathbb{K}} J(\mathbf{v}) \\ \mathbb{K} &= \{ \mathbf{v};\ \operatorname{div} \mathbf{v} = 0,\ \mathbf{v} \cdot \mathbf{n}|_{\Gamma_1} = 0 \} \end{aligned}\right\} \tag{3}$$

Equation (3) can be formulated as a saddle-point problem for the Lagrangian:

$$L(\mathbf{v}, q) = J(\mathbf{v}) + \int_\Omega q \operatorname{div} \mathbf{v} \tag{4}$$

More precisely, $\mathbb{L}^2(\Omega)$ being the space of square integrable functions and $\mathbb{H}^1(\Omega)$ the subspace of $\mathbb{L}^2(\Omega)$ with square integrable first derivatives, we denote

$$\mathbb{H}_{0,\Gamma_2}(\Omega) = \{\varphi \in \mathbb{H}^1(\Omega);\ \varphi|_{\Gamma_2} = 0\}$$

$$\mathbb{H}(\operatorname{div}, \Omega) = \{\mathbf{v} \in (\mathbb{L}^2(\Omega))^d;\ \operatorname{div} \mathbf{v} \in \mathbb{L}^2(\Omega)\}$$

and finally, introducing the space of vector functions such that $\mathbf{v}\cdot\mathbf{n} = 0$ on Γ_1 in a meaningful way, say:

$$\mathbb{H}_{0,\Gamma_1}(\operatorname{div}, \Omega) = \left\{\mathbf{v} \in \mathbb{H}(\operatorname{div}, \Omega);\ \int_\Gamma \mathbf{v}\cdot\mathbf{n}\,\varphi = 0\ \forall \varphi \in \mathbb{H}_{0,\Gamma_2}(\Omega)\right\}$$

We search the couple $(\mathbf{u}, \lambda)$ in $\mathbb{H}_{0,\Gamma_1}(\operatorname{div}, \Omega) \times \mathbb{L}^2(\Omega)$ such that:

$$L(\mathbf{u}, q) \le L(\mathbf{u}, \lambda) \le L(\mathbf{v}, \lambda) \tag{5}$$

for all $\mathbf{q} \in \mathbb{L}^2(\Omega)$ and for all $\mathbf{v} \in \mathbb{H}_{0,\Gamma_1}(\operatorname{div}, \Omega)$, which is characterized by

$$\frac{\partial}{\partial \mathbf{v}} L(\mathbf{u}, \lambda) = 0 \quad \text{and} \quad \frac{\partial}{\partial q} L(\mathbf{u}, \lambda) = 0$$

in other words:

$$\int_\Omega \mathbf{v}^t \mathbf{P}\mathbf{u} + \int_\Omega \lambda \operatorname{div} \mathbf{v} = \int_\Omega \mathbf{v}^t \mathbf{P}\mathbf{u}_0 \tag{6}$$

for all $\mathbf{v} \in \mathbb{H}_{0,\Gamma_1}(\operatorname{div}, \Omega)$, and

$$\int_\Omega q \operatorname{div} \mathbf{u} = 0 \tag{7}$$

for all $q \in \mathbb{L}^2(\Omega)$

Assuming that the Lagrange multiplier λ is sufficiently regular, says $\lambda \in \mathbb{H}^1(\Omega)$, and taking into account eqns (1) and (2) we obtain:

$$\mathbf{u} = \mathbf{u}_0 + \mathbf{P}^{-1}\vec{\nabla}\lambda \quad \text{in} \quad \Omega \tag{8}$$

$$-\vec{\nabla}\cdot(\mathbf{P}^{-1}\vec{\nabla}\lambda) = \vec{\nabla}\cdot\mathbf{u}_0 \quad \text{in} \quad \Omega \tag{9}$$

$$-\mathbf{P}^{-1}\frac{\partial \lambda}{\partial \mathbf{n}} = \mathbf{n}\cdot\mathbf{u}_0 \quad \text{on} \quad \Gamma_1 \tag{10}$$

$$\lambda = 0 \quad \text{on} \quad \Gamma_2 \tag{11}$$

Standard finite element method applied to this problem allows us to calculate the function λ, and from eqn (8) by derivation we get the velocity $\mathbf{u}$.

2.2 *Interpolated field computation*

The field $\mathbf{u}_0$ in eqns (8), (9), and (10) is constructed by interpolation. Let k be the number of observation stations in Ω, then $\mathbf{u}_0$ is given by:

$$\mathbf{u}_0 = \frac{\sum_{j=1}^{k} \mathbf{u}_j \frac{1}{d_j^m}}{\sum_{j=1}^{k} \frac{1}{d_j^m}} \tag{12}$$

where $\mathbf{u}_j$ is the measured velocity in j-th station, $\mathbf{u}_0$ the interpolated velocity in a given point, and d_j the distance from j-th station to that point. In practical applications, the values $m = 1, 2$, and 3 have been chosen in order to analyze the behavior of this parameter.

2.3 *Adaptive strategy*

In the development of *a posteriori* error estimators, three main approaches may be distinguished: Namely, those based on residual, postprocessing, or interpolation techniques. The estimators here follow the first approach.

This first approach began with the work of Babuska and Rheinboldt (1978) and is essentially based on an error equation involving the residual of the computed solution. For triangles of three nodes and linear interpolation, these error indicators are

$$\epsilon_i = \left[\frac{h_i^2}{24\|\mathbf{P}^{-1}\|}\int_{\Omega_i} r^2 d\Omega + \frac{h_i}{24\|\mathbf{P}^{-1}\|}\int_{\Gamma_i}\left[\!\left[[\mathbf{P}^{-1}]\frac{\partial \lambda_h}{\partial n}\right]\!\right]^2 d\Gamma\right]^{1/2} \tag{13}$$

where h_i is the diameter of the Ω_i element having Γ_i boundary; $[\![[\mathbf{P}^{-1}]\frac{\partial \lambda_h}{\partial n}]\!]$ means the jump of the flux associated with the numerical solution λ_h through the boundary Γ_i; r is the residual corresponding to eqn (9). $\|\mathbf{P}^{-1}\|$ stands for a suitable matrix norm of $\mathbf{P}^{-1}$.

A second refinement indicator is:

$$\epsilon_i = h_i|\vec{\nabla}\lambda_h| \tag{14}$$

which allows one to find efficiently the boundary layers that could appear.

Once the error indicators are known, we refine the mesh according to the following strategy: Set $\epsilon_{max} = \max \epsilon_i$ and given the parameter $\gamma \in [0, 1]$ (usually $\gamma \approx 0.2$), we subdivide all the triangles Ω_i which have $\epsilon_i \ge \gamma\epsilon_{max}$.

To refine the mesh we have used the algorithm proposed by Rivara (1984, 1987), which consist basically in the partition of a triangle by means of the introduction of three vertices at the mid points of the three sides and joining the new vertex located on the longest side with the opposite old vertex, and with the other two new vertices. Finally, an additional refinement is performed to assure the conformity of the mesh. Concerning the resolution of the algebraic system of equations, an element-by-element (E.B.E.) conjugate gradient method with diagonal preconditioner has been applied, because of its proven efficiency in many kind

of problems (see Montero *et al.* 1990). We take the solution obtained with a mesh as an initial approximation for the system of equations corresponding to the refined mesh. Furthermore, applying E.B.E. techniques we do not need to stock the global matrix.

2.4 *Applications*

In all the examples, the behaviors of indicators 1 and 2 presented before, eqn (13) and (14) respectively, have been compared. Also, a qualitative difference has been shown between solutions obtained using different interpolations corresponding to the values $m = 1$, 2, and 3 in eqn (12). One step of refinement with a given parameter γ has been made from an initial regular mesh in each example, so that we work with two meshes (first or initial MESH and second MESH). In the next section we show some results using meshes and velocities-field solutions.

2.4.1 *Obstacle model test. Uniform field.* Consider a wind field through a rectangular region with an obstacle in the middle zone, as shown in Fig. 1. The wind velocity is assumed in A, B, C, F, G, and H, and its value is 2 m sec^{-1}, with horizontal direction. In this figure, the impermeable boundary Γ_1 is indicated. Figures 2–5 show the second grid and the solution field obtained by applying Indicator 1 (Babuska indicator) and Indicator 2 (Gradient indicator) to the same initial mesh.

Obviously, we find a better solution of the velocities field by refining the mesh. Indicator 1 introduces fewer elements than the second one.

2.4.2 *Obstacle model test. Non-uniform field.* With the same geometry as the first example, a known wind velocity has been assumed at the points D and E with a value equal to 2.82 m sec^{-1} and a wind direction of 135° and −45° respectively. We have used several numerical strategies as in the first example. In this case, Figs. 6–9 show the corresponding results. Similar conclusions are obtained here, but the refined mesh is non-uniform because of the turbulence of the observed field. Here several refinements allow one to get a better approximation.

2.4.3 *Application in Cañada del Río, Jandía, Island of Fuerteventura.* Finally, the numerical method already described to a real-data case has been applied, concerning the measurement of the meteorological stations in the area of Cañada del Río in Fuerteventura island; see Fig. 10. Table 1 gives the values of measurements of different observations used in this study. We begin with a regular mesh and we perform two refinement steps according to Indicator 1, for different interpolations of the observed field ($m = 1$, 2, or 3). Figures 11–12 show the results using a strategy with $m = 1$. In order to analyze the zones with greater wind power with in the studied domain, the modules of velocities of the solution field are presented, building the contours and their 3-dimensional representation (Fig. 13) for the last refinement step (Mesh 3).

The locations of the zones of greater wind power do not actually depend on the interpolation chosen, although the values of this power change noticeably.

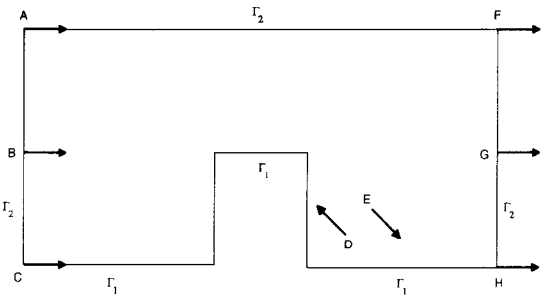

Fig. 1. Obstacle model test.

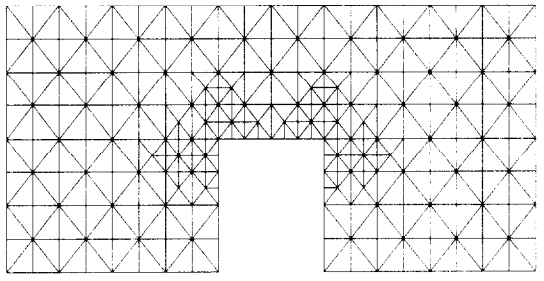

Fig. 2. Second mesh. Babuska indicator.

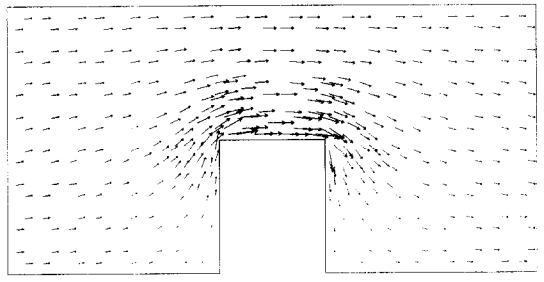

Fig. 3. Second mesh solution. Babuska indicator.

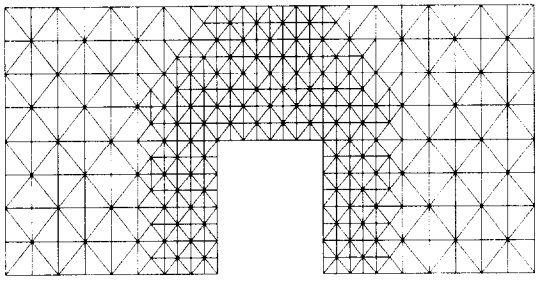

Fig. 4. Second mesh. Gradient indicator.

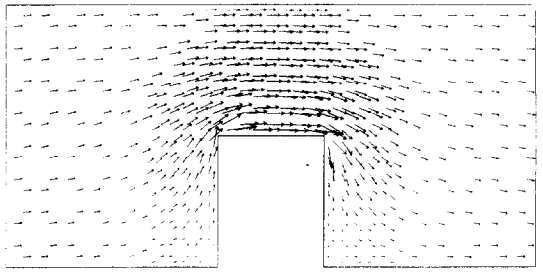

Fig. 5. Second mesh solution. Gradient indicator.

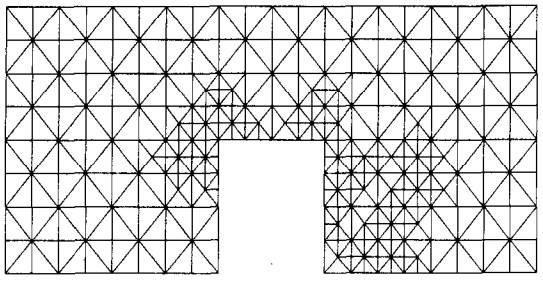

Fig. 6. Second mesh. Babuska indicator.

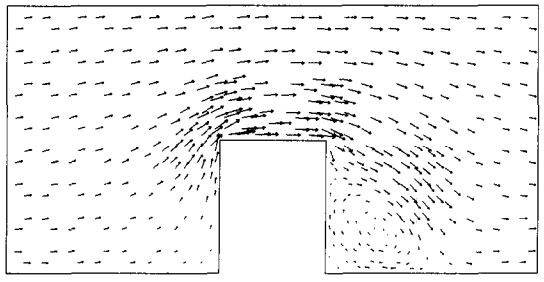

Fig. 7. Second mesh solution. Babuska indicator.

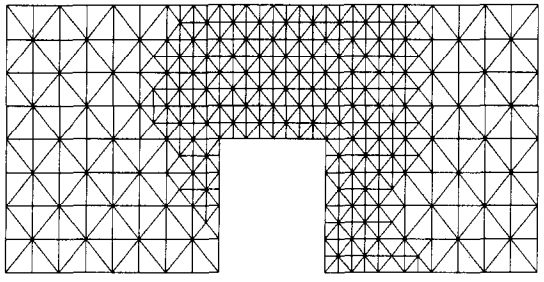

Fig. 8. Second mesh. Gradient indicator.

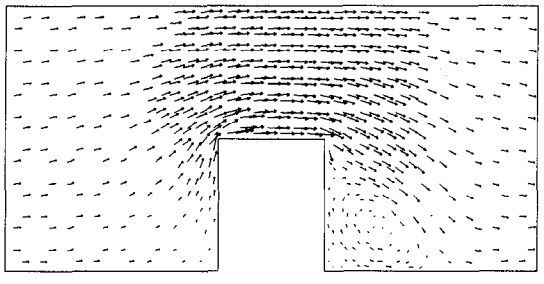

Fig. 9. Second mesh solution. Gradient indicator.

On the other hand, the areas of greatest refinement are the same for the three cases.

3. MIXED FINITE ELEMENT SOLUTION

Following the work of Raviart and Thomas (1977) we consider the direct approximation of eqns (6) and (7): for any integer $k \geq 1$, let $\mathbf{P}_k$ be the space of polynomes of degree k in $\mathbb{R}^d$, and we define

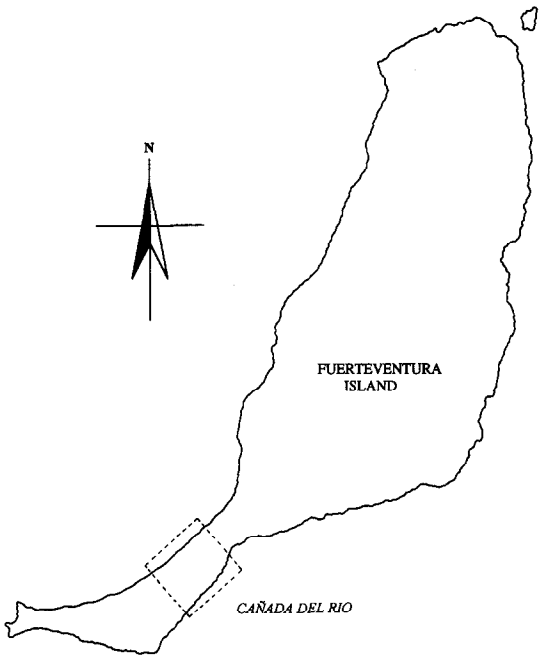

Fig. 10. Fuerteventura Island. Studied domain.

$$D_k = \{\mathbf{v} = (\mathbf{v}_1, \ldots, \mathbf{v}_d);\ \mathbf{v}_i(x) = a_i(x) + x_i a_0(x)$$
$$1 \leq i \leq d \quad \text{with} \quad a_0, a_1, \ldots, a_d \in \mathbf{P}_{k-1}\}$$

We denote $D_k(\tau)$ the restriction of D_k to an element τ of the triangulation T. Now, introducing the finite dimensional spaces

$$X_h = \{\mathbf{v} \in \mathbb{H}_{0,\Gamma_1}(\text{div}, \Omega);\ \mathbf{v}|_\tau \in D_k(\tau) \forall \tau \in T\}$$

$$M_h = \{q \in \mathbb{L}^2(\Omega);\ q|_\tau \in \mathbf{P}_{k-1} \forall \tau \in T\}$$

The approximate problem is:
"Find $(\mathbf{u}_h, \lambda_h) \in X_h \times M_h$ such that

$$\int_\Omega \mathbf{v}^t \mathbf{P} \mathbf{u}_h + \int_\Omega \lambda_h \,\text{div}\, \mathbf{v} = \int_\Omega \mathbf{v}^t \mathbf{P} \mathbf{u}_0 \qquad (15)$$

for all $\mathbf{v} \in X_h$

$$\int_\Omega q \,\text{div}\, \mathbf{u}_h = 0 \qquad (16)$$

for all $q \in M_h$."

Table 1. Observations data

Station	Module km h^{-1}	Direction
1	39.0	209.8°
2	34.2	228.0°
3	32.6	231.2°
4	35.0	253.8°
5	41.4	221.0°
6	30.6	228.3°

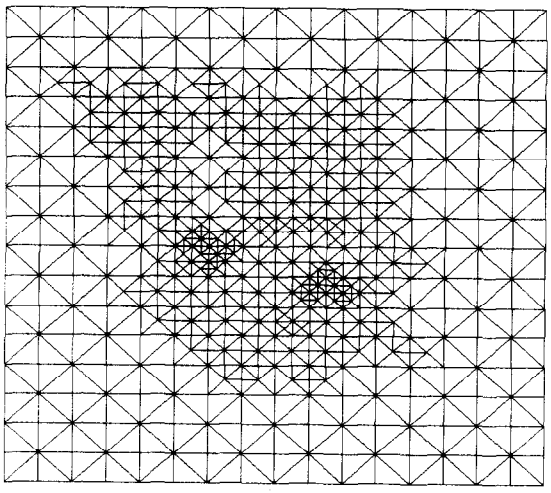

Fig. 11. Cañada del Río application. Third mesh.

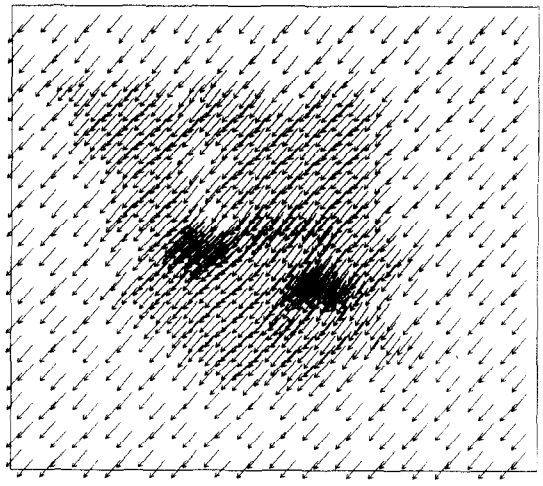

Fig. 12. Cañada del Río application. Third mesh solution.

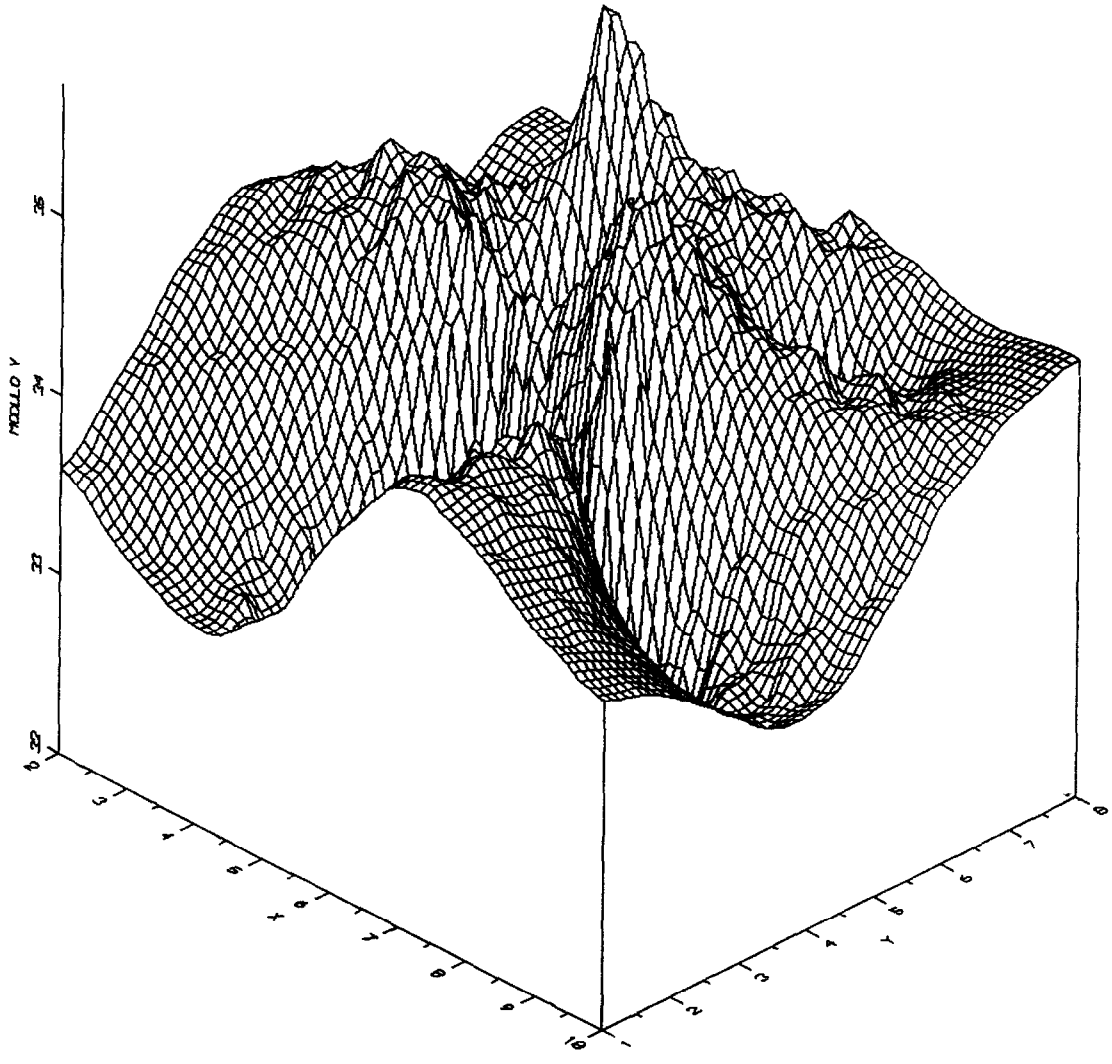

Fig. 13. Cañada del Río application. Modules of velocities in 3D.

We have the following properties for the discrete solution $\mathbf{u}_h$ of eqns (15) and (16):

- continuity of the flows $\mathbf{u}_h \cdot \mathbf{n}$ through the inter-element boundaries, and
- div $\mathbf{u}_h = 0$, as a consequence of eqn (16).

3.1 *Adaptive strategy*

From the continuous eqns (6) and (7) and its discrete version, eqns (15) and (16), we obtain the following *a posteriori* error estimation for the norm:

$$\|\mathbf{v}\| = \left(\int_\Omega \mathbf{v}^t \mathbf{P} \mathbf{v}\right)^{1/2}:$$

$$\|\mathbf{u} - \mathbf{u}_h\| \le \|r\| + C\left(\sum_{\tau'} \|[\lambda_h]\|^2_{1/2,\tau'}\right)^{1/2} \quad (17)$$

where r is given by

$$r = \mathbf{u}_h - \mathbf{u}_0 - \mathbf{P}^{-1}\vec{\nabla}\lambda_h$$

The constant C depending on the $\mathbf{P}$ matrix can be evaluated easily and $[\lambda_h]$ means the jump of λ_h between elements through the sides τ' of the triangulation T. $\|\cdot\|_{1/2,\tau'}$ stands for a proper norm in a trace space.

Using the error estimation, in eqn (17), we consider the error indicator associated to each element τ; for the first order approximation ($k = 1$) we have:

$$\eta_\tau = \left(\int_\tau (\mathbf{u}_h - \mathbf{u}_0)^t \mathbf{P}(\mathbf{u}_h - \mathbf{u}_0)\right)^{1/2} + C\left(\sum_{i=1}^{3} \beta_i [\lambda_i] \text{meas}(\tau')\right)$$

where

$$\beta_i = \begin{cases} 1/2 & \text{if } \tau'_i \cap \Gamma = \varnothing \\ 0 & \text{if } \tau'_i \cap \Gamma_1 \neq \varnothing \\ 1 & \text{if } \tau'_i \cap \Gamma_2 \neq \varnothing \end{cases}$$

In order to define a refinement strategy, in practical computations, we have only considered the first term in η_τ. We refine an element according to the strategy defined in section 2.3, or, alternatively, by setting $\eta^2_{\text{opt}} = \frac{1}{N}\sum \eta^2_\tau$, N being the actual number of elements, we refine the mesh according to the following strategy: (a) if $\eta_\tau \ge \eta_{\text{opt}}$ we refine by four elements, and (b) if $\eta_{\text{opt}} > \eta_\tau \ge 0.5\ \eta_{\text{opt}}$ we refine by two elements. With this kind of subdivision we intend to quickly reach a mesh with uniform error distribution which has been proven to be optimal.

3.2 *Multigrid method*

To solve the mixed variational problem in eqns (15) and (16), we use the multigrid method, see Hackbush (1985), with the sequence of nested subspaces, corresponding to the nested grids generated by the refinement algorithm.

The mixed discrete system corresponding to eqns (15) and (16), can be written in matrix form as:

$$\mathbf{A}\mathbf{u} + \mathbf{B}^t\lambda = \mathbf{b} \quad (18)$$

$$\mathbf{B}\mathbf{u} = 0 \quad (19)$$

We have considered a smoother which could be written as the following Arrow-Hurwicz-Uzawa iteration (see Fortin and Glowinski, 1982):

$$\mathbf{u}^{n+1} = \mathbf{u}^n - \omega S^{-1}(\mathbf{A}_r\mathbf{u}^n + \mathbf{B}^t\lambda^n - \mathbf{b})$$

$$\lambda^{n+1} = \lambda^n + \rho(\mathbf{B}\mathbf{u}^{n+1})$$

where $\mathbf{A}_r = \mathbf{A} + r\mathbf{B}^t\mathbf{B}$, S is an auxiliary operator and ω, ρ are parameters; in our case ωS^{-1} is the operator associated with a few steps of the diagonal preconditioned conjugated gradient method.

Concerning the system in eqns (18) and (19), the restriction and prolongation operator are the L^2 – projection and injection, respectively, for the Lagrange Multiplier λ, as we do not have any continuity requirement for this variable. For the velocities $\mathbf{u}$ we can construct easily the interpolation operator: when we split by its middle point a side of an element, the flow values of the two new sides are taken to be one half of the flow value of their "father"; the values through a new side interior to a triangle can also be calculated using the divergence theorem. The restriction operator

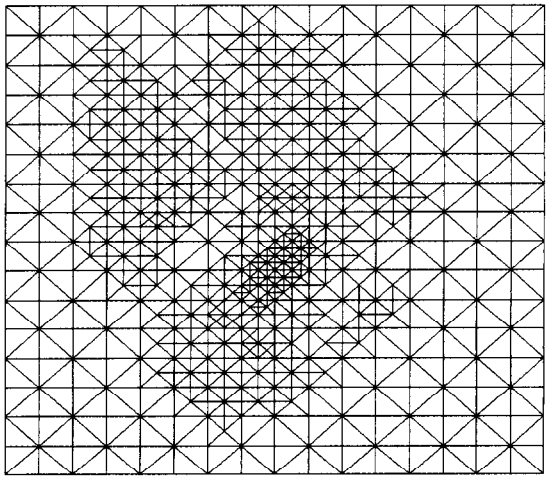

Fig. 14. Cañada del Río application. Third mesh using mixed finite elements.

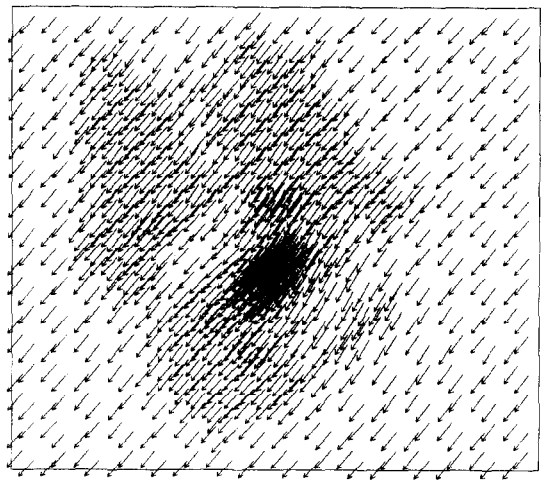

Fig. 15. Cañada del Río application. Third mesh solution using mixed finite elements.

for the flows to pass from a fine grid to a coarser one is straightforward; we only have to sum up the flow values of the two "daughter" sides. For a more detailed analysis see Ferragut *et al.* (1990).

3.3 *New results*

Figures 14–16 show the results obtained for the same application solved in Section 2.4.3, but using the mixed finite element method. In this case we have taken the parameter $m = 2$ for the construction of the interpolated field $\mathbf{u}_0$.

4. CONCLUSIONS

We have presented the development of two numerical methods for wind field adjustment, using a least square procedure, in order to fit the experimental measurements and to meet the incompressibility condition. The corresponding optimization problem is solved by looking for a saddle point of the associated Lagrangian function.

The finite element approximation of the equivalent mixed variational formulation is very suitable as the approximate solution is divergence free. Furthermore, the performance of the adaptive method proposed appears to be very satisfying both from a numerical point of view and that of computational efficiency. Finally, the result obtained in the real data Fuerteventura case has been accepted as reasonable and will be used as input data in a further energy resources estimation.

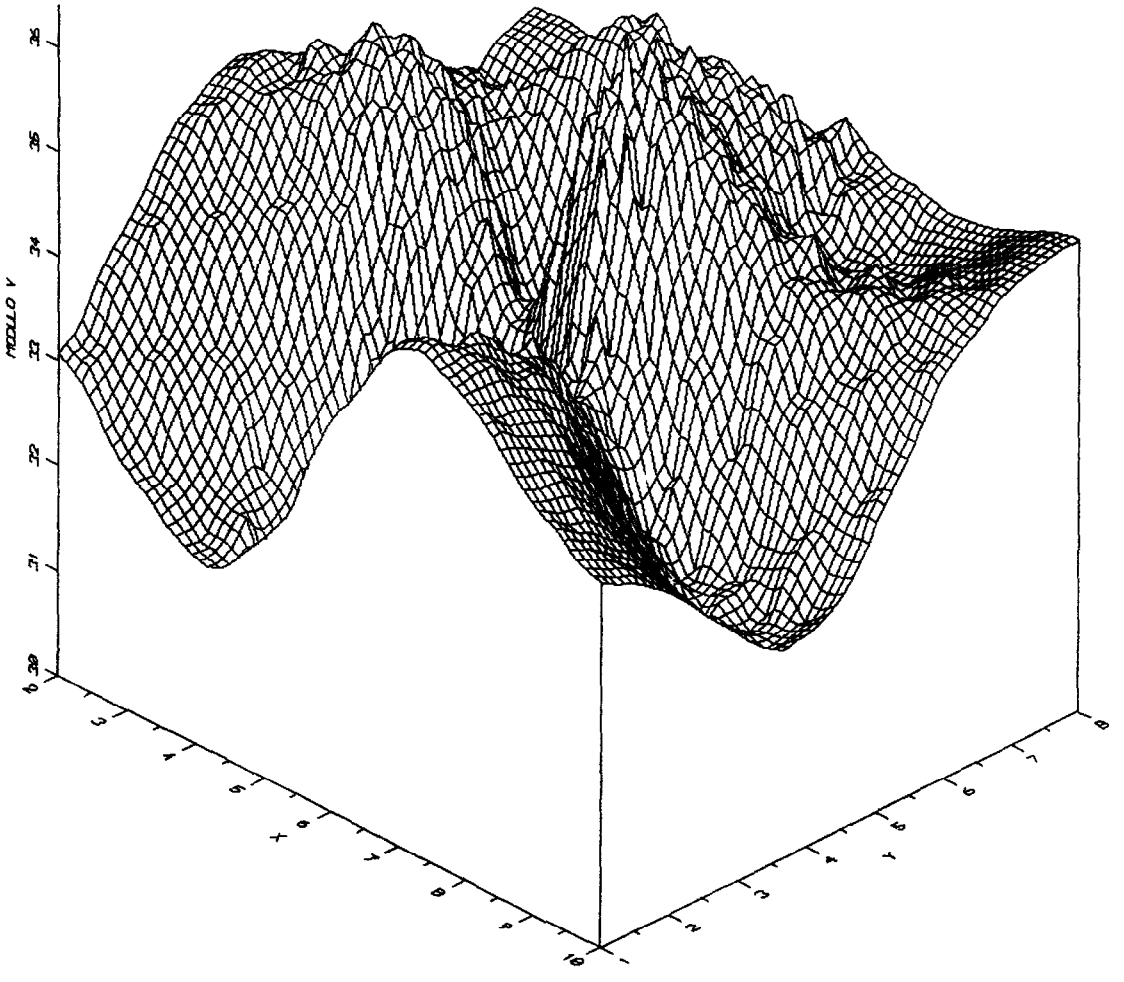

Fig. 16. Cañada del Río Application. Modules of velocities in 3D using mixed finite elements.

Acknowledgments—This research has been sponsored in part by the Consejería de Industria y Energía del Gobierno de Canarias.

REFERENCES

L. Adell, R. Zubiaur, F. Martin, F. Ferrando, P. Moreno, L. Varona, and A. Pantoja, Development of a methodology for the estimation of wind energy resources in relatively large areas: Application to the eastern and central parts of Spain, *Solar Energy* **38**, 281–295 (1987).

I. Babuska, J. Chandra, and J. E. Flaherty, *Adaptive computational methods for partial differential equations*, SIAM, Philadelphia (1983).

I. Babuska and W. C. Rheinboldt, Error estimates for adaptive finite element computations, *Siam J. Numer. Anal.* **15**, 736–754 (1978).

J. Y. Caneill, P. Racher, and R. Rosset, *A finite-element formulation of a* variational *procedure of wind-field adjustment over complex terrain*, Electricite de France, Direction des Estudes et Recherches (1984).

L. Ferragut, R. Montenegro, G. Montero, and G. Winter, Ajuste de un campo de viento mediante elementos finitos mixtos, *Memorias I Congreso Métodos Numéricos en Ingenería*, 90–95, Las Palmas de Gran Canaria (1990).

M. Fortin and R. Glowinski, *Methodes de Lagrangien Aumenté*, Dunod, Paris (1982).

E. Fraga, J. Hernandez, and A. Crespo, Modelización del flujo del viento basada en la conservación de la masa, *Anal. Ing. Mec.* **3**(1) (1985).

W. Hackbush, *Multigrid methods and applications*, Springer-Verlag, Berlin (1985).

G. Montero, R. Montenegro, G. Winter, and L. Ferragut, Aplicación de esquemas EBE en procesos adaptativos, *Rev. Int. Met. Num. Cal. Dis. Ing.* **6**, 311–332 (1990).

P. A. Raviart and J. M. Thomas, *A mixed finite element method for second order elliptic problems*, Mathematical Aspects of Finite Element Method, Lecture Notes in Math. 606, Springer-Verlag, Berlin (1977).

M. C. Rivara, A grid generator based on 4-triangles conforming. Mesh refinement algorithms, *Int. J. Numer. Meth. in Eng.* **24**, 1343–1354 (1987).

M. C. Rivara, Algorithmics for refining triangular grids suitable for adaptive and multigrid techniques, *Int. J. Num. Meth. Eng.* **20**, 745–756 (1984).

C. A. Sherman, A mass consistent model for wind fields over complex terrain, *J. Appl. Meteor.* **17**, 312–319 (1978).